Mild mitochondrial uncoupling impacts cellular aging in human muscles *in vivo*

Catherine E. Amara*, Eric G. Shankland*, Sharon A. Jubrias*, David J. Marcinek*, Martin J. Kushmerick*†‡, and Kevin E. Conley*†‡§

Departments of *Radiology, †Physiology and Biophysics, and ‡Bioengineering, University of Washington Medical Center, Seattle, WA 98195

Communicated by Ewald R. Weibel, University of Bern, Bern, Switzerland, November 16, 2006 (received for review July 22, 2006)

Faster aging is predicted in more active tissues and animals because of greater reactive oxygen species generation. Yet age-related cell loss is greater in less active cell types, such as type II muscle fibers. Mitochondrial uncoupling has been proposed as a mechanism that reduces reactive oxygen species production and could account for this paradox between longevity and activity. We distinguished these hypotheses by using innovative optical and magnetic resonance spectroscopic methods applied to noninvasively measured ATP synthesis and O_2 uptake *in vivo* in human muscle. Here we show that mitochondrial function is unchanged with age in mildly uncoupled tibialis anterior muscle (75% type I) despite a high respiratory rate in adults. In contrast, substantial uncoupling and loss of cellular [ATP] indicative of mitochondrial dysfunction with age was found in the lower respiring and well coupled first dorsal interosseus (43–50% type II) of the same subjects. These results reject respiration rate as the sole factor impacting the tempo of cellular aging. Instead, they support mild uncoupling as a mechanism protecting mitochondrial function and contributing to the paradoxical longevity of the most active muscle fibers.

magnetic resonance spectroscopy | optical spectroscopy | oxidative phosphorylation

The rate-of-living hypothesis proposes that higher rates of oxidative metabolism cause an increased production of reactive oxygen species (ROS) (1), leading to oxidative damage and mitochondrial dysfunction with age. However, mice with the lowest resting respiration rate have been shown to have the shortest longevity (2). Similarly, isolated muscle fibers show greater generation of ROS in type II fibers (3), which have the lowest oxidative capacity and chronic activity levels. This fiber type also has the shortest longevity and is the first to be lost with age (4). Thus, the tempo of aging appears to vary among mice and muscle fiber types but in an opposite manner than predicted by the rate-of-living hypothesis, with the least active having the shortest longevity.

A physiological mechanism that could account for this paradox is mild mitochondrial uncoupling, which has been proposed to ameliorate ROS production by reducing reverse electron flow and superoxide generation (5). Consistent with this prediction are findings in mice with high respiration rates that showed elevated proton leak in isolated muscle mitochondria as a result of activation of the adenine nucleotide translocator and uncoupling protein 3. Mild uncoupling resulting from activation of these mitochondrial factors in type I muscle fibers could reduce ROS production, protect mitochondria from damage, and account for the longevity of this fiber type with age. A number of studies have provided evidence of mild uncoupling in human muscles (6, 7) but have not tested whether this uncoupling protects against mitochondrial dysfunction and cellular aging.

New methods permit measurement of mitochondrial coupling *in vivo* by using a combination of noninvasive spectroscopic techniques (8, 9). Recently developed magnetic resonance spectroscopy (MRS) tools have demonstrated mitochondrial uncoupling *in vivo* in human muscle with thyroid hormone treatment (10) and in mouse muscle containing uncoupling protein 3 (11). A pairing of optical spectroscopy and MRS permits a quantitative measure of coupling (P/O, which is half the ratio of ATP flux to O_2 uptake) and has revealed substantial uncoupling in mouse hindlimb muscles *in vivo* when treated with a chemical uncoupler (8) and with age (12). These noninvasive methods allow us to quantitatively evaluate the presence and extent of uncoupling *in vivo* as a function of age in human muscles not typically studied by invasive methods. These methods also make possible a test for cellular aging by using a drop in muscle [ATP] or energy charge ([ATP]/[ADP]) as a measure of the first step in the cell death cascade (13). [ATP] depletion is associated with impairment of ion pumps that leads to membrane rupture and cell death, which is an important contributor to sarcopenia (14).

Here, we apply these tools to test (*i*) whether mild uncoupling is found in human muscle comprised of predominantly type I vs. type II fibers and (*ii*) the impact of uncoupling on cellular aging as measured by muscle [ATP] depletion. Resting muscle metabolism is measured to avoid the confounding effects of energetic differences between fiber types during exercise to permit focusing on mitochondrial energetics and the impact of uncoupling on cellular aging.

Results

Absolute Quantification. Table 1 lists the intracellular high-energy phosphate and O_2 carrier concentrations for the adult and elderly groups. The phosphocreatine (PCr) level in the adult group was close to values determined by chemical analysis of biopsy tissue from adult human quadriceps ([PCr] = 29 mM and [ATP] = 6.8 mM) (15). Similarly, the values for myoglobin (Mb) intermuscular concentration, [Mb], fell within a range of concentrations (0.26–0.52 mM) in tissue biopsies taken from adult quadriceps muscles (16–18). Most of the age-related differences were either not significant or small (<15%). The small age-related changes, due to the increased muscle cell water that occurs with age (19), were eliminated by normalizing [ATP] and [Mb] to [PCr]. An exception was [ATP]/[PCr] in the first dorsal interosseus (FDI), which suggests that [ATP] in this muscle is reduced with age. A paired *t* test revealed a significantly lower [ATP] in the FDI than in the tibialis anterior (TA) in the elderly ($P < 0.011$, paired *t* test), despite similar levels in the two adult muscles ($P > 0.14$, paired *t* test). Thus, our marker of cellular

Author contributions: C.E.A., E.G.S., D.J.M., M.J.K., and K.E.C. designed research; C.E.A., E.G.S., and S.A.J. performed research; C.E.A., E.G.S., S.A.J., and K.E.C. analyzed data; and K.E.C. wrote the paper.

The authors declare no conflict of interest.

Freely available online through the PNAS open access option.

Abbreviations: ROS, reactive oxygen species; MRS, magnetic resonance spectroscopy; PCr, phosphocreatine; P/O, half the ratio of ATP flux to O_2 uptake; Mb, myoglobin; FDI, first dorsal interosseus; TA, tibialis anterior.

§To whom correspondence should be addressed at: Department of Radiology, Box 357115, University of Washington Medical Center, Seattle, WA 98195-7115. E-mail: kconley@u.washington.edu.

This article contains supporting information online at www.pnas.org/cgi/content/full/0610131104/DC1.

Table 1. Cellular high-energy phosphates and O_2 carriers in the FDI and TA muscles of the two age groups

	FDI		TA	
Compound	Adult	Elderly	Adult	Elderly
[PCr]	28.0 ± 1.0	24.5 ± 1.3*	28.6 ± 1.1	25.5 ± 1.8*
[ATP]	6.3 ± 0.4	4.5 ± 0.2*	7.0 ± 0.2	5.6 ± 0.2*
[ATP]/[PCr]	0.22 ± 0.01	0.18 ± 0.01*	0.24 ± 0.01	0.22 ± 0.01
[ADP]	0.027 ± 0.002	0.032 ± 0.004	0.025 ± 0.002	0.029 ± 0.004
[P_i]	3.4 ± 0.4	2.4 ± 0.2	3.1 ± 0.2	2.9 ± 0.2
[Mb]	0.27 ± 0.01	0.24 ± 0.01*	0.44 ± 0.02	0.36 ± 0.05*
[Mb]/[PCr]	0.0096 ± 0.0003	0.0103 ± 0.0008	0.016 ± 0.001	0.013 ± 0.001
[Hb]	0.02 ± 0.01	0.03 ± 0.01	0.09 ± 0.02	0.17 ± 0.06*

Values are shown as the means ± SEM of millimolar concentrations. *, Significant difference between adult and elderly groups.

aging was significantly changed in contrast to other metabolites in the FDI, whereas [ATP] was relatively unaltered in the TA between adult and elderly muscle.

O_2 Uptake. The optical spectroscopic measurements shown in Fig. 1 distinguishing Mb and hemoglobin (Hb) O_2 saturation (Fig. 1 *Upper*) were used to determine O_2 uptake during the initial period of ischemia. The O_2 uptake in the adult FDI muscle (1.4 ± 0.1 $\mu M \cdot sec^{-1}$) was in good agreement with traditional, invasive measurements of O_2 uptake from blood reported for resting forearm muscles [1.0 ± 0.4 (SD) $\mu M \cdot sec^{-1}$; using the Fick method] (20, 21). Fig. 2*a* shows that the O_2 uptake of the TA was significantly higher than that of the FDI in the adults.

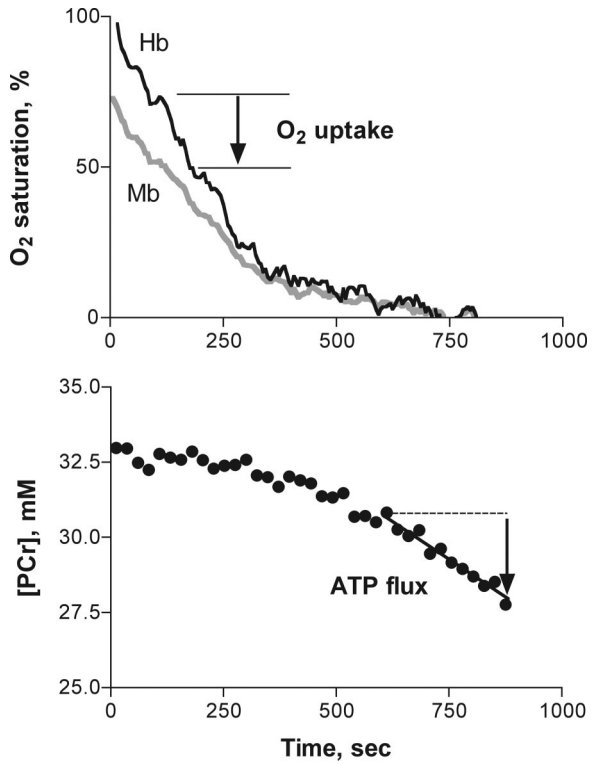

Fig. 1. Spectroscopic measurements during ischemia that yield O_2 uptake, ATP flux, and energy coupling (P/O) in an adult human TA muscle at rest. (*Upper*) An optical spectroscopic measurement distinguishing Mb and Hb O_2 saturation that is used with their respective *in vivo* concentrations (Table 1) to determine O_2 uptake during the initial period of ischemia. (*Lower*) MRS measurement of the dynamics of [PCr]. The [PCr] breakdown during ischemia measures ATP turnover by the cell that must be met by ATP supply from the mitochondria under aerobic conditions.

Net ATP Turnover and Mitochondrial ATP Supply. The ATP flux was determined by MRS with the dynamics and concentration of the high-energy phosphate carrier PCr during anoxia in the muscle (Fig. 1). Because glycolytic ATP synthesis generates PCr (via the creatine kinase reaction), the measured PCr breakdown (ΔPCr) reflects the difference between glycolytic synthesis and the ATP turnover by the cell. Thus, the net ATP turnover that must be met by the mitochondria under aerobic conditions is measured by ΔPCr during ischemia. Fig. 2*b* shows that the average net ATP turnover met by mitochondrial ATP synthesis in the adults did not differ between the FDI and TA. Our independent measurement of glycolysis (FDI: H^+ flux at 0.30 ± 0.08 $\mu M \cdot sec^{-1}$, TA: H^+ flux at 0.60 ± 0.36 $\mu M \cdot sec^{-1}$) indicates that <8% of total ATP turnover in the cell is met by this ATP supply pathway in the adults (assuming $PCr/H^+ = 1$ for glucose uptake as the source of substrate level phosphorylation).

A significantly reduced net ATP turnover is evident in the elderly group relative to adults in each muscle. A similar drop in oxidative ATP flux with age was reported in human soleus muscle by an independent MRS method *in vivo* (22). However, there was no significant change in the glycolytic ATP synthesis with age in either muscle or in the contribution of this pathway to the total ATP turnover in the elderly muscles (FDI: H^+ flux at 0.22 ± 0.10 $\mu M \cdot sec^{-1}$, TA: H^+ flux at 0.32 ± 0.20 $\mu M \cdot sec^{-1}$). Thus >92% of the ATP supply in the resting muscle cell in adult or elderly humans is provided by mitochondrial respiration as measured by net ATP turnover.

Energy Coupling. Combining measurements of O_2 flux with ATP flux yielded a direct measurement of energy coupling or P/O in adult human FDI *in vivo* (mean: 2.68 ± 0.05), as shown in Fig. 2*c* for the adult and elderly subjects. The P/O in the muscles of the adult group is close to the value for oxidative phosphorylation coupling reported for intact cells and isolated human mitochondria ($P/O \approx 2.3$–2.5) (23, 24). This correspondence with the values in the literature as well as the small variance among adult subjects indicates that mitochondria in the FDI are well coupled in the adults. In contrast, reduced coupling was apparent in the TA ($P/O = 2.0 \pm 0.2$) in this study and significantly differed from that in the FDI by $\Delta P/O = 0.7$. Thus, the lower P/O in the TA suggests mild uncoupling of oxidative phosphorylation as compared with the well coupled FDI.

A decline in coupling was apparent in the FDI muscles of the elderly group. The average P/O for this group ($P/O = 1.6 \pm 0.2$) was 40% less than the adult value. In contrast, there was no difference in the mild uncoupling state in the TA between the

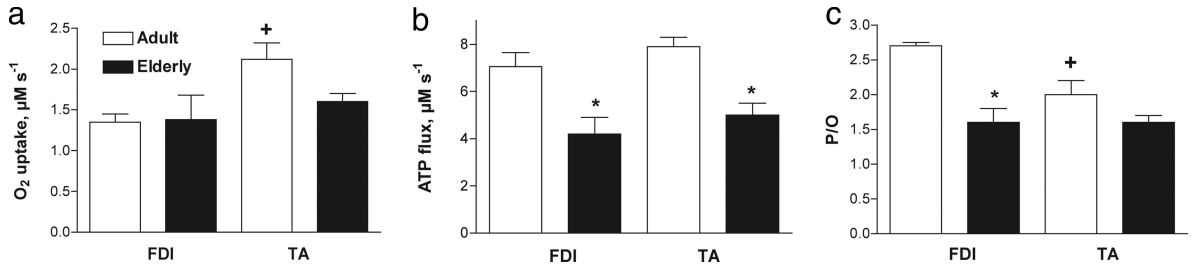

Fig. 2. Energy fluxes used to determine mitochondrial coupling in FDI and TA muscles of adult and elderly subjects. (*a*) Oxygen uptake rates. (*b*) Oxidative phosphorylation rates (ATP flux). (*c*) Coupling of oxidation to phosphorylation (P/O). +, significant difference between adult TA and adult FDI; *, significant difference between adult and elderly values of each muscle.

adult and elderly subjects ($\Delta P/O = 0.5$). Thus, the TA had higher resting O_2 uptake in the adults but little change in coupling with age. In contrast, the FDI had lower O_2 uptake in the adults but showed significant reduction in coupling and depletion of cellular [ATP] with age.

[ATP] vs. P/O. A significantly lower [ATP] was found in the FDI vs. TA of the elderly ($P < 0.011$, paired t test), despite similar levels in the adult muscles ($P > 0.14$, paired t test). [ATP] was proportional to mitochondrial coupling in the FDI ($r^2 = 0.42$, $P < 0.004$). However, there was no correlation between [ATP] and P/O for the TA ($r^2 = 0.04$) and mild uncoupling was not accompanied by reduced [ATP] in the adult TA muscle (Table 1).

Discussion

Mitochondria are a key source of the ROS causing age-related damage. The rate-of-living hypothesis states that respiration rate sets the pace of ROS production (1), whereas recent results find that the highest rates of ROS generation occur in well coupled mitochondria at low levels of respiration (14). Here we show that mitochondrial coupling level rather than respiration rate has the greatest impact on cellular aging. The FDI muscle with the lower rate of respiration but highest coupling level showed significant mitochondrial dysfunction with age. In contrast, little age-related mitochondrial dysfunction or [ATP] depletion was found with mild uncoupling in the TA despite its higher respiration rate. These results support mild uncoupling as a protective mechanism that minimizes ROS production in adult tissue and preserves mitochondrial function with age.

Comparing the rate of respiration and coupling level between muscles was possible by the combined measurement of O_2 flux and ATP flux, as shown in Fig. 1. The O_2 uptake was determined during the first minute of ischemia over a P_{O_2} range that we have shown in mice *in vivo* (41) and others have shown in human muscle *in vivo* (25) to not impair mitochondrial respiration (i.e., Mb-O_2 > 50% saturated and $P_{O_2} > 3$ torr). The desaturation kinetics (Fig. 1) and chromophore levels (Table 1) yielded rates of O_2 uptake that were significantly higher in the TA than in the FDI in the adults (Fig. 2*A*). However, no difference was found in the ATP flux (Fig. 2*B*) determined by MRS based on the dynamics and concentration of PCr during anoxia in the muscle (Fig. 1). This similarity in muscle ATP turnover at rest reflects the fact that cell ATP turnover at rest is governed by the Na-K-ATPase and protein synthesis, which are not expected to vary greatly among muscle fibers (26). In contrast, activation of the myosin ATPases results in large differences in ATP turnover between muscle fiber types during exercise. Mouse muscles representing the extremes of fiber type composition, showed the same energetic fluxes at rest but greater than the 2-fold differences in flux during exercise at the same stimulation rate (27). Thus, eliminating contractile energetic differences by studying resting muscle reveals little difference in ATP turnover but does reveal a significant difference in mitochondrial O_2 uptake between muscles of the same subject.

A simple ATP balance approach provided the measure of mitochondrial ATP synthesis *in vivo*. Eliminating oxidative phosphorylation by anoxia permitted the use of PCr breakdown to measure the net cell ATP turnover that the mitochondria meets under resting, oxygenated conditions. Validation of this approach comes from a direct comparison of mitochondrial respiration under aerobic conditions vs. net ATP turnover during anoxia in isolated mouse muscles (27) and *in vivo* in rattlesnake tailshaker muscle (28). Anoxia of up to 30 min in intact muscle does not impact the activity of a key ATPase in resting muscle, Na-K-ATPase (29), and our measurements of glycolysis indicate a negligible contribution to ATP supply during the anoxic period (<8%). Thus, brief anoxia appears to not affect cell ATP use nor raise glycolysis, which allows us to use the ATP turnover as a measure of the mitochondrial ATP generation under aerobic conditions.

The difference in O_2 uptake but similar ATP flux in the two muscles yielded a higher P/O in the FDI as compared with the TA of the adult group (Fig. 2*c*). The P/O of the FDI is close to independent measurements (P/O = 2.5) in intact cells in vastus lateralis muscle (30) and skin fibroblasts (31) from humans. In contrast, reduced coupling was apparent in the TA (P/O = 2.0) in this study and differed from that in the FDI by $\Delta P/O = 0.7$. A difference in substrate oxidation could account for part of this P/O difference: Oxidizing palmitate vs. pyruvate would reduce coupling by 0.2–0.3 (23). The large disparity in coupling that remains between muscles reflects a greater O_2 uptake at similar ATP flux in the TA vs. FDI and is consistent with the physiological adjustment that occurs with chemical uncoupling, as shown by the mouse hindlimb *in vivo* after administration of dinitrophenol (8). Thus the lower P/O in the TA appears to be largely due to mild uncoupling of oxidative phosphorylation as compared with the well coupled FDI.

Evidence that regulation of H^+ transport is responsible for mild mitochondrial uncoupling and the disparity in resting respiration between muscles comes from a comparison of mitochondrial function in two groups of mice differing in respiration rate (2). Mitochondria isolated from the high resting respiration group had increased proton leak due to fatty acid activation of the adenine nucleotide transporter and uncoupling protein 3, two key sources of H^+ transport across the inner mitochondrial membrane (23). In contrast, significantly less H^+ transporter activation was found in mitochondria from the low respiration group. Fatty acid activation of the uncoupling protein 3 and adenine nucleotide translocator could also underlie the increased respiration and uncoupling in TA vs. FDI found in this study because higher intracellular lipid levels are reported in type I fibers of human muscle (32).

We tested for the impact of mild uncoupling in adults on mitochondrial function with age by using [ATP] as a measure of cellular aging. A significantly lower cellular [ATP] was found in

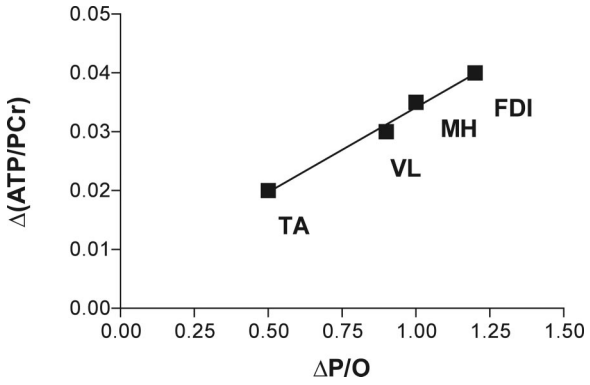

Fig. 3. Mitochondrial changes with age measured as depletion of [ATP] (Δ[ATP]/[PCr]) versus energy uncoupling (ΔP/O) in TA and FDI (this study), vastus lateralis (VL) (15), and mouse hindlimb muscles (MH) (12).

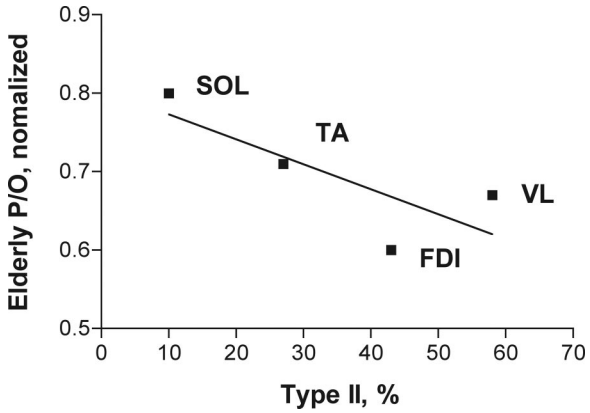

Fig. 4. Uncoupling of muscle in elderly human muscles as a function of percent type II fiber content [soleus (SOL) (22), TA and FDI (this study), and vastus lateralis (VL) (15); muscle fiber type content is from Johnson *et al.* (50)]. Relative uncoupling with age is determined by normalizing the elderly coupling value to the adult value to permit the comparison studies using different methodologies.

the FDI vs. TA of the elderly, despite similar levels in the adult muscles. A substantial reduction in P/O of the FDI of the elderly subjects (ΔP/O = 1.2) from the well coupled level in the adults accompanied this loss of cellular [ATP]. A disparity in energetic changes between muscles also is reported in aged rats with ATP depletion and reduced ATP synthesis occurring in the gastrocnemius (high percentage of type II fibers) but not in the heart (33). The chronic activity decline typical with age would be expected to affect the leg muscle (TA) and not the hand muscle (FDI) and therefore does not account for the aging effects seen in this study.

A pairing of the depletion of the cellular energy state (reduced [ATP] or [ATP]/[ADP]) and mitochondrial dysfunction with age as seen in the FDI has been reported in human vastus lateralis (15) and mouse hindlimb muscles (12). Fig. 3 shows that [ATP] normalized to [PCr] was depleted in proportion to the drop in mitochondrial coupling with age in these muscles. This pairing of reduced cellular [ATP] with uncoupling is consistent with a shift in the equilibrium relationship among energy coupling, mitochondrial membrane potential (Δp), and the cellular phosphorylation state (34). With chemical uncoupling or mild uncoupling in the adult TA, cellular phosphorylation state is maintained by an elevation of O_2 uptake (and electron transport chain flux) in response to increased H^+ leak and decreased Δp. In contrast, uncoupling with age is not compensated by increased O_2 uptake in the FDI (Fig. 2*A*) or in the hindlimb of elderly mice (12). This uncompensated uncoupling would impact the cellular phosphorylation state, and because [ADP] and [P_i] are unchanged this impact is seen as a depletion of muscle [ATP] (Table 1). Thus, a shift in cellular phosphorylation state resulting in muscle [ATP] depletion is what distinguishes the large drop in coupling with age from the mild uncoupling in the TA vs. FDI of the adults.

Uncoupling with age is thought to result from accumulation of ROS damage to the inner mitochondrial membrane, causing increased H^+ leak (35) in contrast to the transporter-mediated (adenine nucleotide translocator or uncoupling protein 3) H^+ leak in adult mitochondria (23). Thus, the cause of uncoupling likely also differs between adult and elderly muscle. The cellular [ATP] depletion accompanying age-related uncoupling in aged FDI muscle is consistent with a shift in the energetic equilibrium between the mitochondria and cell, but it is also possible that [ATP] depletion reflects an independent site of mitochondrial damage with age. Two recent reports identify oxidative damage at the site of phosphorylation, the ATP synthase (36, 37). In either case, an energetic shift or oxidative damage to the ATP synthase, the resulting loss of cellular [ATP] is critical to the fate of the cell by initiating the cell death cascade (14). Thus, the age-related [ATP] depletion in the FDI may represent a first step in the processes that trigger apoptotic and necrotic pathways and therefore may be responsible for the preferential fiber loss in type II fibers with age.

This stability of mitochondrial coupling and [ATP] relative to other metabolites (Table 1) in the TA with age suggests that mild uncoupling in the adult is protective against mitochondrial dysfunction into old age (38). The mechanism of this protection is a reduction in reverse electron flux with mild uncoupling that results in lower ROS generation, as found in isolated mitochondria (5, 39). One site of oxidative damage by ROS is the inner mitochondrial membrane, which is thought to underlie the increased H^+ leak and uncoupling found with age. Reduction in ROS by mild uncoupling in adult muscle is a mechanism that would minimize membrane damage and further uncoupling in old age. In support of this model is the greater longevity of mice with higher resting O_2 uptake and mitochondrial H^+ leak. The stable mitochondrial and cell energy state evident in the TA with age may well reflect the impact of lower ROS generation reported in type I muscle fibers of adult rat muscle (3) and may be responsible for the greater longevity characteristic of this fiber type in elderly human muscle (4).

A role for muscle fiber type as a factor in mitochondrial uncoupling with age is evident in Fig. 4. This plot shows the degree of uncoupling expressed as the elderly human P/O value normalized to the adult human value to permit comparing studies using different methodologies. The decline in age-related function is smallest in the soleus muscle (22), which contains predominantly type I fibers, and increases with the percentage of type II fiber content in the muscle. This variation in the mitochondrial function with the fiber type composition of muscle likely reflects the metabolic properties associated with muscle fiber types (e.g., type I is slow-twitch and oxidative). Higher intracellular lipid in type I fibers (32) is an example of a factor that could be responsible for the mild uncoupling in adults that in turn leads to preservation of mitochondrial function with age in type I fibers. Thus, mitochondrial dysfunction in elderly human muscle varies with fiber type content just as has been found for ROS generation and the longevity of muscle fibers (3). Mild uncoupling that reduces mitochondrial and cellular energetic changes with age, as found in this study in the predominantly type I TA, provides a mechanism for the fiber type dependence of these age-related dysfunctions.

This study found the least mitochondrial dysfunction in muscles expected to show the greatest age-related damage according to the rate of living hypothesis (1). Muscle with the most active fiber type and higher resting O_2 uptake had mild uncoupling in adults but stable mitochondrial function into old age. This protection of mitochondrial function suggests that mild uncoupling is a mechanism that reduces the ROS production, ameliorates mitochondrial damage, and assists fiber survival with age. In contrast, muscle with greater content of the least active fiber type (type II) and lower resting O_2 uptake was well coupled in adults yet showed changes in mitochondrial coupling and depletion of [ATP] with age consistent with ROS damage. Thus, mild uncoupling may explain the paradox of greater longevity in the most active fibers by providing a protective mechanism that impacts the pace of cellular aging.

Materials and Methods

Subjects. Eleven adult subjects ≤50 yr old (19–50 yr) constituted the adult group (four female and seven male). This age range was selected to exclude subjects likely to have significant functional changes as found in hand muscles of subjects older than 60 yr (40). Eight elderly subjects from 67 to 85 yr old were studied (three female and five male). All subjects were recreationally active, with the exception an adult amateur athlete and one sedentary elderly individual. The two groups were of similar height (177 ± 7 vs. 174 ± 9 cm; adult vs. elderly) and had similar weight (76 ± 8 vs. 78 ± 15 kg). All subjects voluntarily gave informed, written consent, and the study was approved by the University of Washington Human Subjects Review Committee. This study was undertaken in accordance with the Declaration of Helsinki.

Experimental Design. Three design features underlie the measurement of mitochondrial function *in vivo* [see the supporting information (SI)]. First, our measurements focus on mitochondrial energetics under resting conditions to avoid contractile energetic differences between muscles. Second, reversible ischemia is used to block blood flow and permit separating O_2 uptake from ATP flux, as we have described (8). We use the deoxygenation of Mb and Hb determined by optical spectroscopy to measure O_2 uptake in muscle (41), as shown in Fig. 1 *Upper*. In this experiment, O_2 uptake is determined from the drop in O_2 content of each carrier (Δ% saturation × concentration) during ischemia. The desaturation rate is determined during the first minute of ischemia, when Mb-O_2 is >50% saturated (P_{O_2} > 3 torr) and mitochondrial respiration is independent of cellular P_{O_2} (8). Third, the rate of mitochondrial ATP supply is determined by using an ATP balance approach. Once oxidative ATP supply ceases due to lack of oxygen (time = 600 s in Fig. 1), the breakdown of PCr (ΔPCr) provides the ATP supply for the needs of the cell via the creatine kinase reaction (see the SI) as shown in Fig. 1 *Lower*. This ΔPCr represents the net ATP turnover of the resting cell (total ATP use minus glycolytic ATP supply), which the mitochondria must synthesize under aerobic conditions (net ATP turnover equals oxidative ATP supply) (see the SI; see also ref. 28). Thus, a simple ischemic protocol paired with noninvasive spectroscopic tools measures O_2 uptake as well as the ATP flux that must be synthesized by the mitochondria *in vivo*.

Protocols. The basic protocol and measurements have been described for mouse hindlimb muscle (8, 12). The first step was to determine absolute concentrations of PCr and ATP in resting muscle by ^{31}P MRS. The second step was an ischemia protocol that consisted of an aerobic rest period followed by rapid inflation of a cuff to 55 mmHg (1 mmHg = 133 Pa) above systolic blood pressure that was maintained for 15 min. During the first minute, the dynamics of Mb-O_2 and Hb-O_2 saturation were measured. The cell was anoxic by 10 min of ischemia. The PCr and pH dynamics were determined for the last 3 min of the protocol. To scale the Hb and Mb saturation, the subjects breathed 100% O_2 in the optical experiments starting 5 min before ischemia and continuing until the end of the 12–16 min of recovery. No hyperoxic breathing was used during the MRS measurements because the PCr level was unaffected by breathing of 100% O_2 and ΔPCr was determined during cell anoxia. The third step was to determine the level of [Hb] and [Mb] in the ischemic muscle. Optical measurement of [Hb]/[Mb] was made during the final minute of ischemia. A separate ischemic experiment was used to quantify [Mb] and involved 2 min of exercise to rapidly deplete O_2 and fully desaturate Mb. Serial acquisition of the deoxy-Mb peak with ^{1}H MRS during the remaining several minutes of ischemia ensured that full desaturation was achieved. The individual spectra that were fully desaturated were summed to maximize the signal-to-noise ratio of the final peak for analysis.

MRS. All MRS experiments were performed in a Bruker (Billerica, MA) 4.7-T short bore magnet with a Varian (Palo Alto, CA) Inova (imaging/spectroscopy) console. Details of our methods are published (42), and the specific procedures for the FDI and TA appear in ref. 43 (see also the SI). The concentrations of PCr, ATP, and Mb in muscle were determined by comparison against external standards (44). Free [ADP] was calculated from the creatine kinase equilibrium with correction of the equilibrium constant for pH (45).

Measurement of Net ATP Turnover. A detailed description of the procedure for measuring resting ATP flux was given in our original papers on this method in human muscle (42). Briefly, the rate of PCr breakdown (ΔPCr) in anoxic muscle was used to measure the net ATP turnover, which represents the basal ATP use of the cell minus the glycolytic ATP supply. This ΔPCr is the flux that must be met by mitochondrial oxidative phosphorylation under aerobic condition to achieve an ATP balance. To independently access the contribution of glycolysis to cellular ATP supply, the rate of glycolytic ATP production was determined by using the change in pH and PCr during ischemia, as previously described (46). Validation of this approach *in vivo* is given in ref. 28. Repeated measures of muscle ATP flux on the same subject agreed to within ±11% (47).

Optical Spectroscopy. Two 6.4-mm fiberoptic bundles (model no. G39–368; Edmund Optics, Barrington, NJ) with a fixed separation distance (1.9 cm, FDI; 2.2 cm, TA) were positioned adjacent to one another over the muscle. Care was taken to ensure full contact between the probes and the skin throughout the experiment. One fiber carrying white light from a quartz–tungsten halogen source (model no. TS-428; Acton Research/Roper Scientific, Trenton, NJ) illuminated the tissue. The remaining fiber carried reflected light to a spectrograph (CP200 part no. 31 027 668; ISA Division, Jobin-Yvon Longjumeau, France) mounted to a 512- × 512-pixel, front-illuminated CCD detector (512 TEK/1UV; Princeton Instruments, Trenton, NJ) and connected to a controller (ST-135; Princeton Instruments). A 133 g/mm grating coupled to a 190-cm focal length spectrograph was used to obtain spectra over the range of wavelengths from 488 to 953 nm. We used a 200-ms exposure time and a 9-s delay between scans, resulting in a data acquisition rate of ≈1 spectra per 10.1 s. Our approach for developing calibration sets and for the PLS analysis of the spectra has been described in detail for mouse hindlimb muscle *in vivo* (41).

Normalizing saturation. The two-point calibration for O_2 saturation has been described for mouse muscle *in vivo* (41). The peak Hb-O_2 saturation level was established by breathing 100% O_2. Mb and Hb saturation curves were normalized so that the last 2

min of ischemia represented 0% saturation (Fig. 1). Release of the cuff caused a rapid reoxygenation and the peak (≈30 s) of the hyperemic response was used to calculate 100% saturation. The Hb]/[Mb] in muscle was determined by using the spectral position of the combined Mb and Hb deoxy peak in the *in vivo* spectrum, as described for heart tissue (48). The [Hb] was calculated from the optical determination of [Hb]/[Mb] and the [Mb] measured by ^{1}H MRS.

Determining O_2 uptake. The O_2 uptake was determined from deoxygenation of Hb-O_2 and Mb-O_2 during the first minute of ischemia, when Mb-O_2 is >50% saturated ($P_{O_2} > 3$ torr) and mitochondrial respiration is independent of cellular P_{O_2} (Fig. 1), as previously described (8, 41). A linear regression of the depletion of these O_2 stores vs. time was used to measure the rate of O_2 uptake by the mitochondria (8).

Mitochondrial Energy Coupling (P/O). The ratio of net ATP turnover to O_2 uptake was divided by 2 to yield P/O to conform with biochemical convention. Coupling was calculated for the vastus lateralis from the phosphorylation capacity per mitochondrial volume reported in the vastus lateralis muscle (15). Oxygen uptake was calculated by using the maximum O_2 uptake rate per mitochondrial volume (5 ml of O_2 per milliliter of mitochondria per minute (49), which was converted to concentration units by using 0.05 μM O_2 per percentage of mitochondria in muscle.

Statistics. Means were compared by using a Newman–Kuels test. Paired, two-tailed *t* tests were used to compare the muscle and age-effect on [ATP] with significance assigned at the 0.025 level with a Bonferroni correction. Linear regressions were performed to determine the rate of change of Mb-O_2 and Hb-O_2 (O_2 uptake) and PCr content (net ATP turnover). Pearson correlations were performed to test the relationship between independent variables. Significance was assigned at the 0.05 level unless noted otherwise.

We thank Lori Arakaki, Wayne Ciesielski, David Niles, and Ken A. Schenkman for their contributions. This work was supported by National Institutes of Health Grants R01 AR 41928, R01 AR 45184, R01 AR 36281, and R01 AG-022385 and by National Institutes of Health Training Grant AG00057.

1. Beckman KB, Ames BN (1998) *Physiol Rev* 78:547–581.
2. Speakman JR, Talbot DA, Selman C, Snart S, McLaren JS, Redman P, Krol E, Jackson DM, Johnson MS, Brand MD (2004) *Aging Cell* 3:87–95.
3. Anderson EJ, Neufer PD (2006) *Am J Physiol* 290:C844–C851.
4. Lexell J (1995) *J Gerontol* 50A:11–16.
5. Echtay KS, Roussel D, St-Pierre J, Jekabsons MB, Cadenas S, Stuart JA, Harper JA, Roebuck SJ, Morrison A, Pickering S, *et al*. (2002) *Nature* 415:96–99.
6. Fernstrom M, Tonkonogi M, Sahlin K (2004) *J Physiol* 554:755–763.
7. Schrauwen P, Hesselink M (2003) *Proc Nutr Soc* 62:635–643.
8. Marcinek DJ, Schenkman KA, Ciesielski WA, Conley KE (2004) *Am J Physiol* 286:C457–C463.
9. Marcinek DJ (2004) *Acta Physiol Scand* 182:343–352.
10. Lebon V, Dufour S, Petersen KF, Ren J, Jucker BM, Slezak LA, Cline GW, Rothman DL, Shulman GI (2001) *J Clin Invest* 108:733–737.
11. Cline GW, Vidal-Puig AJ, Dufour S, Cadman KS, Lowell BB, Shulman GI (2001) *J Biol Chem* 276:20240–20244.
12. Marcinek DJ, Schenkman KA, Ciesielski WA, Lee D, Conley KE (2005) *J Physiol* 569:467–473.
13. Borutaite V, Brown GC (2003) *Free Radical Biol Med* 35:1457–1468.
14. Skulachev VP (2006) *Apoptosis* 11:473–485.
15. Conley KE, Jubrias SA, Esselman PE (2000) *J Physiol* 526:203–210.
16. Nemeth P, Lowry O (1984) *J Histochem Cytochem* 32:1211–1216.
17. Sylven C, Jansson E, Böök K (1984) *Cardiovasc Res* 18:443–446.
18. Moller P, Sylven C (1981) *Scand J Clin Lab Invest* 41:479–482.
19. Proctor DN, O'Brien PC, Atkinson EJ, Nair KS (1999) *Am J Physiol* 277:E489–E495.
20. Zurlo F, Larson K, Bogardus C, Ravussin E (1990) *J Clin Invest* 86:1423–1427.
21. Van Beekvelt MC, Colier WN, Wevers RA, Van Engelen BG (2001) *J Appl Physiol* 90:511–519.
22. Petersen KF, Befroy D, Dufour S, Dziura J, Ariyan C, Rothman DL, DiPietro L, Cline GW, Shulman GI (2003) *Science* 300:1140–1142.
23. Brand MD (2005) *Biochem Soc Trans* 33:897–904.
24. Nicholls D, Ferguson S (2002) *Bioenergetics 3* (Academic, London).
25. Haseler LJ, Hogan MC, Richardson RS (1999) *J Appl Physiol* 86:2013–2018.
26. Rolfe DF, Brown GC (1997) *Physiol Rev* 77:731–758.
27. Crow MT, Kushmerick MJ (1982) *J Gen Physiol* 79:147–166.
28. Kemper WF, Lindstedt SL, Hartzler LK, Hicks JW, Conley KE (2001) *Proc Natl Acad Sci USA* 98:723–728.
29. Okamoto K, Wang W, Rounds J, Chambers EA, Jacobs DO (2001) *Am J Physiol* 281:E479–E488.
30. Kuznetsov AV, Kunz WS, Saks V, Usson Y, Mazat JP, Letellier T, Gellerich FN, Margreiter R (2003) *Anal Biochem* 319:296–303.
31. Greco M, Villani G, Mazzucchelli F, Bresolin N, Papa S, Attardi G (2003) *FASEB J* 17:1706–1708.
32. Howald H, Hoppeler H, Claassen H, Mathieu O, Straub R (1985) *Pflügers Arch* 403:369–376.
33. Drew B, Phaneuf S, Dirks A, Selman C, Gredilla R, Lezza A, Barja G, Leeuwenburgh C (2003) *Am J Physiol* 284:R474–R480.
34. Nicholls DG (2004) *Aging Cell* 3:35–40.
35. Harper ME, Bevilacqua L, Hagopian K, Weindruch R, Ramsey JJ (2004) *Acta Physiol Scand* 182:321–331.
36. Mansouri A, Muller FL, Liu Y, Ng R, Faulkner J, Hamilton M, Richardson A, Huang TT, Epstein CJ, Van Remmen H (2006) *Mech Ageing Dev* 127:298–306.
37. Yarian CS, Rebrin I, Sohal RS (2005) *Biochem Biophys Res Commun* 330:151–156.
38. Brand MD (2000) *Exp Gerontol* 35:811–820.
39. Brand MD, Buckingham JA, Esteves TC, Green K, Lambert AJ, Miwa S, Murphy MP, Pakay JL, Talbot DA, Echtay KS (2004) *Biochem Soc Symp*, 203–213.
40. Narici M, Bordini M, Cerretelli P (1991) *J Appl Physiol* 71:1277–1281.
41. Marcinek DJ, Ciesielski WA, Conley KE, Schenkman KA (2003) *Am J Physiol* 285:H1900–H1908.
42. Blei ML, Conley KE, Kushmerick MJ (1993) *J Physiol* 465:203–222.
43. Jubrias SA, Crowther GJ, Shankland EG, Gronka RK, Conley KE (2003) *J Physiol* 553:589–599.
44. Buchli R, Boesiger P (1993) *Magn Reson Med* 30:552–558.
45. Golding EM, Teague WE, Dobson GP (1995) *J Exp Biol* 198:1775–1782.
46. Conley KE, Blei ML, Richards TL, Kushmerick MJ, Jubrias SA (1997) *Am J Physiol* 273:C306–C315.
47. Blei ML, Conley KE, Odderson IB, Esselman PC, Kushmerick MJ (1993) *Proc Natl Acad Sci USA* 90:7396–7400.
48. Territo PR, Balaban RS (2000) *Anal Biochem* 286:156–163.
49. Hoppeler H (1990) *Respir Physiol* 80:137–145.
50. Johnson M, Polgar J, Weightman D, Appleton D (1973) *J Neurol Sci* 18:111–129.